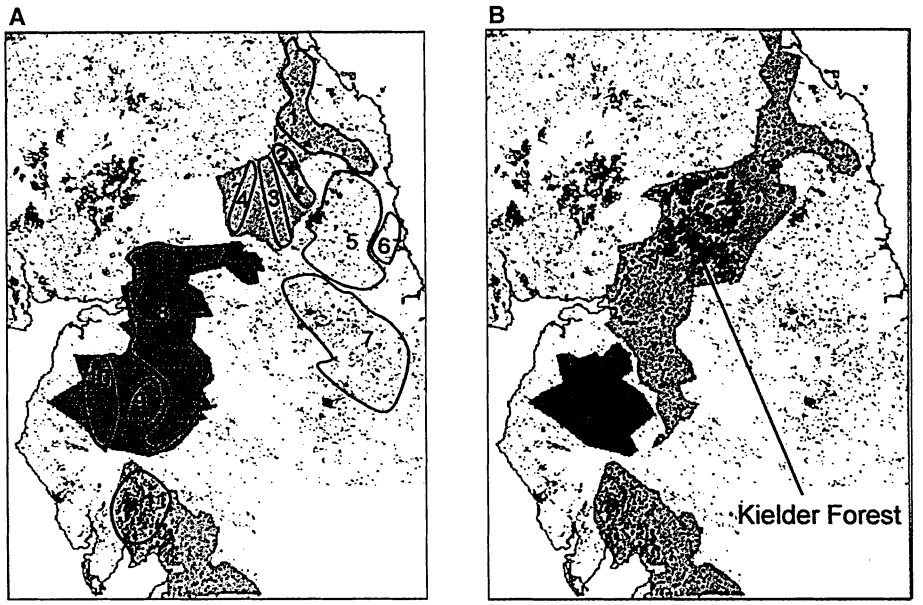

Fig. 3. Change in genetic composition and woodland coverage. (**A**) Woodland coverage in the absence of Kielder Forest is represented in dark green, with the three basic red squirrel genetic groups color coded. Red = northern group: Ford (1) (n = 4 individuals), Harwood (2) (n = 2), Sidwood (3) (n = 2), and Wauchope (4) (n = 2), plus Foulshaw Moss (11) (n = 5). Yellow = eastern group: Rothbury (5) (n = 10), Morpeth (6) (n = 2), and Tyne Valley (7) (n = 30). Blue = western group: Cumbria (8) (n = 31), Pooley Bridge (9) (n = 2), and Rosthwaite (10) (n = 2). The colored areas include all woods within the linking distance of 1.5 km to woods where squirrels were sampled. Black outlines indicate the area over which specimens in each population were collected. (**B**) Woodland coverage including Kielder Forest. Again, the three main groups are color coded as above. Cumbria (8) now forms part of the northern genetic group.

Our study takes advantage of large changes in habitat fragmentation and accurate maps and samples over the same period, enabling us to show the importance of habitat patches in wild populations as avenues for dispersal. The northern genes have leapfrogged through hundreds of forest fragments in a period of 20 years, demonstrating the use of stepping stone patches of forest by red squirrels. These findings suggest that where a network of stepping stones is available within a critical dispersal distance, gene flow can be very rapid through highly fragmented landscapes. It also indicates that human-made changes affecting the connectivity of a landscape can result in changes in genetic structure, not only in the area of habitat change but in populations hundreds of kilometers from the site of habitat change.

References and Notes

1. T. M. Caro, M. K. Laurenson, *Science* **263**, 485 (1994).
2. R. Lande, S. Shannon, *Evolution* **50**, 434 (1996).
3. M. Bevers, C. H. Flather, *Theor. Pop. Biol.* **55**, 61 (1999).
4. N. Haddad, *Conserv. Biol.* **14**, 738 (2000).
5. J. Gurnell, P. W. W. Lurz, Eds., *The Conservation of Red Squirrels*, Sciurus vulgaris L. (Peoples Trust for Endangered Species, London, 1997).
6. P. W. W. Lurz, thesis, University of Newcastle, Newcastle-upon-Tyne, UK (1995).
7. The *Land Cover Map of Great Britain* (*14*) provided remotely sensed habitat data for all woodlands on a 25-m grid-based (raster) format for the sample region.
8. R. McIntosh, *For. Ecol. Manage.* **79**,1 (1995).
9. M. L. Hale, R. Bevan, K. Wolff, *Mol. Ecol. Notes* **1**, 47 (2001).
10. Supplemental Web material is available on *Science* Online at www.sciencemag.org/cgi/content/full/293/5538/2246/DC1.
11. L. A. Wauters, P. Casale, A. A. Dhondt, *Oikos* **69**, 140 (1994).
12. L. A. Wauters, in (*5*), pp. 5–12.
13. Woodland habitat patches were classed as separate if they were divided by a minimum of 25 m of non-woodland habitat, and the sample region encompassed a total of 171 676 individual woodlots. These woodland data were stored in GRASS, a Geographic Information System (GIS). We investigated landscape connectivity across the sample region by analyzing the spatial separation of individual patches of woodland by nonforested habitats using a custom-built C program linked to the GIS in a Unix-shell environment. The program interrogated a position list of habitat patches in the landscape collated from the GIS. All woodland patches that were separated by a distance less than the defined connecting distance were assigned to the same woodland group.
14. R. M. Fuller, G. B. Groom, A. R. Jones, *Photo. Eng. Remote Sens.* **60**, 553 (1994).
15. S. Schneider, D. Roessli, L. Excoffier, *ARLEQUIN version 2000: A Software for Population Genetics Data Analysis* (see http://anthro.unige.ch/arlequin) (2000).
16. O. E. Gaggiotti, O. Lange, K. R. Rassmann, C. A. Gliddon, *Mol. Ecol.* **8**, 1513 (1999).
17. D. Paetkau, W. Calvert, I. Stirling, C. Strobeck, *Mol. Ecol.* **4**, 347 (1995).
18. D. Paetkau, L. P. Waits, P. L. Clarkson, L. Craighead, C. Strobeck, *Genetics* **147**, 1943 (1997).
19. P. M. Waser, C. Strobeck, *Trends Ecol. Evol.* **13**, 43 (1998).
20. Genotype assignment was calculated were the program available at www.biology.ualberta.ca/jbrzusto/Doh.php.
21. J. D. Matthews, *Production of Seed by Forest Trees in Britain* (Forestry Commission Report on Forest Research 1954, Her Majesty's Stationery Office, London, 1955), pp. 64–78.
22. P. W. W. Lurz, P. J. Garson, S. P. Rushton, *For. Ecol. Manage.* **79**, 79 (1995).
23. J. M. Tonkin, thesis, University of Bradford, Bradford, UK (1983).
24. J. C. Reynolds, *J. Anim. Ecol.* **54**, 149 (1985).
25. P. Beier, R. F. Noss, *Conserv. Biol.* **12**, 1241 (1998).
26. T. H. Keitt, D. L. Urban, B. T. Milne, *Conserv. Ecol.* (online) **1**, 4 (1997).
27. M. Nei, *Am. Nat.* **106**, 283 (1972).
28. J. Felsenstein, *PHYLIP* (*Phylogeny Inference Package*) *version 3.5c* (distributed by the author) (Department of Genetics, Univ. of Washington, Seattle, WA, 1993).
29. R. D. M. Page, *Comp. Appl. Biosci.* **12**, 357 (1996).
30. M. Shorten, *Squirrels* (Collins, London, 1954).

31. We thank the Hancock Museum in Newcastle and the Tullie House Museum in Carlisle for access to their skin collections, and C. Brummer, E. Morton, and S. Hewitt for their personal support of the project. Funded by the University of Newcastle-upon-Tyne.

16 May 2001; accepted 9 August 2001

Effects of Size and Temperature on Metabolic Rate

James F. Gillooly,[1]* James H. Brown,[1,2] Geoffrey B. West,[2,3] Van M. Savage,[2,3] Eric L. Charnov[1]

We derive a general model, based on principles of biochemical kinetics and allometry, that characterizes the effects of temperature and body mass on metabolic rate. The model fits metabolic rates of microbes, ectotherms, endotherms (including those in hibernation), and plants in temperatures ranging from 0° to 40°C. Mass- and temperature-compensated resting metabolic rates of all organisms are similar: The lowest (for unicellular organisms and plants) is separated from the highest (for endothermic vertebrates) by a factor of about 20. Temperature and body size are primary determinants of biological time and ecological roles.

Metabolism sustains life. It is the process by which energy and materials are transformed within an organism and exchanged between the organism and its environment. Whole organism metabolic rate scales with the 3/4-power of body mass and increases exponentially with temperature (*1*, *2*). The effect of temperature on a biological process is tradi-

tionally expressed as a Q_{10}, which quantifies temperature dependence across a limited temperature range (i.e., 10°C).

Size and temperature primarily affect metabolic rate through different mechanisms. Recently, a general model has been shown to explain the scaling of whole organism metabolic rate B with body mass M, where $B \propto M^{3/4}$ so that mass-specific metabolic rate $B/M \propto M^{-1/4}$. This quarter-power scaling is based on the fractal-like design of exchange surfaces and distribution networks in plants (*3*) and animals (*4*). Temperature governs metabolism through its effects on rates of biochemical reactions. Reaction kinetics vary with temperature according to the Boltzmann's factor $e^{-E_i/kT}$, where T is the absolute temperature (in degrees K), E_i is the activation energy, and k is Boltzmann's constant.

Metabolic rate is the consequence of many different biological reactions. So

$$B = \sum_i R_i$$

where the R_i represents the rates of energy production via the individual reactions (i) that comprise metabolism. Each reaction rate depends on three major variables: $R_i \propto$ (concentration of reactants) (fluxes of reactants) (kinetic energy of the system). The first two terms, which are constrained by the rates of supply of substrates and removal of products, contain the majority of the body mass dependence. Because of allometric constraints on exchange surfaces and distribution networks (*3*, *4*), the product of these two terms scales with body size as $M^{3/4}$. The third term contains the dominant temperature dependence, which is governed by the Boltzmann factor, $e^{-E_i/kT}$. This is valid within the limited range of "biologically relevant" temperatures between approximately 0° and 40°C. This is the range that organisms commonly operate within under natural conditions. Near 0°C, metabolic reactions cease due to the phase transition associated with freezing water, and above approximately 40°C, metabolic reaction rates are reduced by the increasing influence of catabolism. We do not consider hyperthermaphiles, specialized organisms that live at temperatures substantially hotter than 40°C.

The combined effects of body size and temperature on metabolic rate within the biologically relevant temperature range can therefore be well approximated by

$$B \sim M^{3/4} e^{-E_i/kT} \quad (1)$$

Here E_i represents an average activation energy for the rate-limiting enzyme-catalyzed biochemical reactions of metabolism. Because, for each taxon, $B/M^{3/4} = B_0$ is approximately independent of M, almost all of the temperature variation is contained in the normalization term, B_0

$$B_0 \sim e^{-E_i/kT} \quad (2)$$

Because the biochemistry of metabolism is common to aerobic organisms, we predict that plotting mass-normalized metabolic rates [$\ln(B_0)$] as a function of $1/T$ for different taxonomic or functional groups should yield similar straight lines with slopes, $a = -E_i/k$. Furthermore, we predict that the values of E_i obtained from these plots will fall within the range of measured activation energies for metabolic reactions. Because these activation energies vary between 0.2 and 1.2 eV with an average of approximately 0.6 eV (*5*, *6*), the slope of these lines should have a universal value of approximately –7.40 K.

We evaluated these predictions using resting metabolic rates as a function of temperature and body mass for a variety of organisms: aerobic microbes, plants, multicellular invertebrates, fishes, amphibians, reptiles, birds, and mammals (Fig. 1) (*7*). Plots of these data are well fit by straight lines, all with similar slopes and intercepts. This supports the first prediction. Furthermore, the average activation energies extracted from the slopes give $E_i = 0.41 - 0.74$ eV with a mean for all groups of 0.62 eV. This supports the second prediction. Figure 1 suggests that as a first approximation the metabolic rates of all organisms are a single, general function of body size and temperature. An expression for the dependence of metabolic rate on body size and temperature can be derived from Eq. 2 by noting that the value of B_0 at some temperature T can be related to its value at some other temperature T_0 by

$$B_0(T) = B_0(T_0)e^{-E_i/k(1/T - 1/T_0)} = B_0(T_0)e^{E_i(T-T_0)/kTT_0}$$

Combined with Eq. 1 this leads to

$$B = B_0(T)M^{3/4} = B_0(T_0)M^{3/4}e^{E_iT_c/kTT_0} \quad (3)$$

where $T_c = T - T_0$. The term $e^{E_iT_c/kTT_0} = e^{E_iT_c/\{kT_0^2(1+T_c/T_0)\}}$, which describes the "universal temperature dependence" (UTD) of biological processes. Equation 3 allows metabolic rates of different organisms to be compared independently of body mass and temperature by comparing their values of $B_0(T_c)$ normalized with some standard temperature, T_c (often 20°C).

Equation 3 also expresses the temperature dependence in terms of degrees Celsius by choosing T_0 to be the freezing point of water (~273 K), in which case $T_c = T - T_0$ defines temperature in degrees Celsius. Biologists would be better served by quantifying temperature-dependence in terms of the UTD rather than the traditional Q_{10} factor, which is defined by the equation

$$\frac{B_0(T)}{B_0(T_0)} = [Q_{10}]^{(T-T_0)/10} = [Q_{10}]^{T_c/10} \quad (4)$$

with Q_{10} considered a constant, which is independent of temperature. From Eq. 3, however, we see that Q_{10} must, in fact, have a temperature dependence given by

$$Q_{10} = e^{10E_i/kTT_0} = e^{10E_i/\{kT_0^2(1+T_c/T_0)\}} \quad (5)$$

In other words, biological processes do not generally depend purely exponentially on

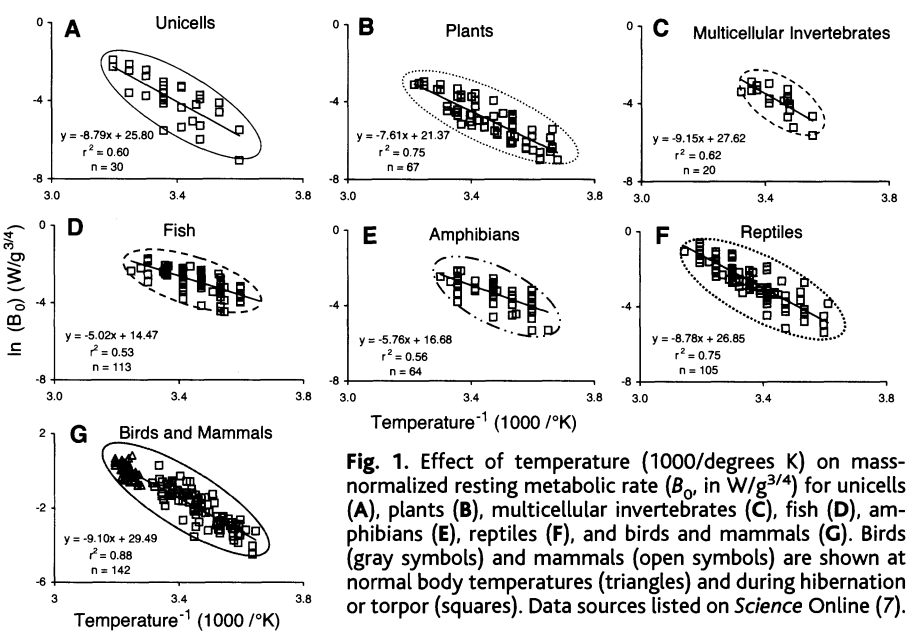

Fig. 1. Effect of temperature (1000/degrees K) on mass-normalized resting metabolic rate (B_0, in W/g$^{3/4}$) for unicells (**A**), plants (**B**), multicellular invertebrates (**C**), fish (**D**), amphibians (**E**), reptiles (**F**), and birds and mammals (**G**). Birds (gray symbols) and mammals (open symbols) are shown at normal body temperatures (triangles) and during hibernation or torpor (squares). Data sources listed on *Science* Online (*7*).

[1]Department of Biology, The University of New Mexico, Albuquerque, NM 87131, USA. [2]Santa Fe Institute, 1399 Hyde Park Road, Santa Fe, NM 87501, USA. [3]Theoretical Division, MS B285, Los Alamos National Laboratory, Los Alamos, NM 87545, USA.

*To whom correspondence should be addressed. E-mail: gillooly@unm.edu

temperature (in degrees Celsius). Calculating temperature dependence using Eq. 4 with a constant value of Q_{10} introduces an error that can be as much as 15% over the "biologically relevant" temperature range. Using the UTD not only avoids this error, but also expresses temperature dependence in terms of the activation energy E_i and Boltzmann's constant k, thereby linking whole-organism metabolism directly to the kinetics of the underlying biochemical reactions.

Because biological times are the reciprocals of biological rates per unit mass, Eq. 1 can be rewritten to give a general expression for biological time (t_b) in terms of body size and temperature

$$t_b \propto M^{1/4}\, e^{E_i/kT} \qquad (6)$$

Eq. 6 should apply to all biological times, from times of biochemical reactions and cell cycles to developmental times and life-spans. Thus, we predict that plots of ln ($t_b M^{-1/4}$) as a function of $1000/T$ should yield straight lines with slopes identical in magnitude but opposite in sign to the plots of ln(B_0) as a function of $1000/T$ for each group (Fig. 1). Plots of life-spans (LS) of fish and aquatic invertebrates of varying body sizes measured at different constant temperatures support this prediction (Fig. 2) (*7*). The slopes for life-span are 6.37 and 6.50 for fish and aquatic invertebrates, respectively, compared with slopes of –5.02 and –9.15 for metabolic rate. The approximately opposite slopes mean that over the lifetime of these animals a unit of mass uses approximately the same quantity of energy, regardless of body size and temperature.

This is not meant to imply that Eq. 1 can account for all variation in biological rates and times. There is residual variation about the lines in Fig. 1 that reflects differences among species. Moreover, the data that we compiled are for resting metabolic rates. Rates of metabolism for endotherms during maximal aerobic activity can be as much as 8- to 10-fold greater than those at rest (*8*). Furthermore, in response to stressful environmental conditions, some organisms have metabolic rates below normal resting levels (e.g., diapause, anhydrobiosis) (*9*). We regard Eq. 1 as the zeroeth-order model that describes the effects of size and temperature as primary. Other, secondary factors are required to explain the remaining variation within and between groups.

The general application of Eq. 1 is demonstrated by the diversity of organisms depicted in Fig. 1. The unicells include protists, algae, and bacteria. The data for plants include not only whole plants, but also fruits, storage organs (tubers, bulbs), and hydrated seeds. Botanists rarely measure rates of whole-plant photosynthesis or respiration as a function of "body" size and temperature [but see (*10*)]. These results suggest that metabolic rates of plants are similar to those of unicellular organisms and invertebrate animals. The data for birds and mammals include not only resting individuals of many species at normal body temperatures, but also individuals in hibernation or torpor at lower body temperatures. These last data imply that the lower metabolic rates of torpid endotherms can be attributed to temperature, as long as body temperatures approximate ambient temperatures; there is no need to invoke other mechanisms to reduce metabolic rate during torpor (*11*).

The primary effects of size and temperature and the residual variation due to other factors can be shown by comparing metabolic rates as a function of temperature and body mass (Fig. 3). Three results are apparent. First, the slopes are similar (Fig. 3A) for all groups except fish and amphibians, which appear to have slopes which are slightly less negative, and consequently also have lower intercepts. Second, the average relations for the different groups are offset somewhat (Fig. 3A). The maximum difference separating any of the groups, unicells and plants from birds and mammals, is approximately e^3 or 20-fold. Third, these differences are small compared with variation in measured values within the groups (Fig. 3B). The data points for each group in Fig. 1 overlap broadly across groups, calling attention to the similarity in metabolic rates of all organisms.

This similarity is perhaps best depicted by plotting whole-organism metabolic rates, corrected to a common temperature of 20°C, as a function of body mass (*12*).

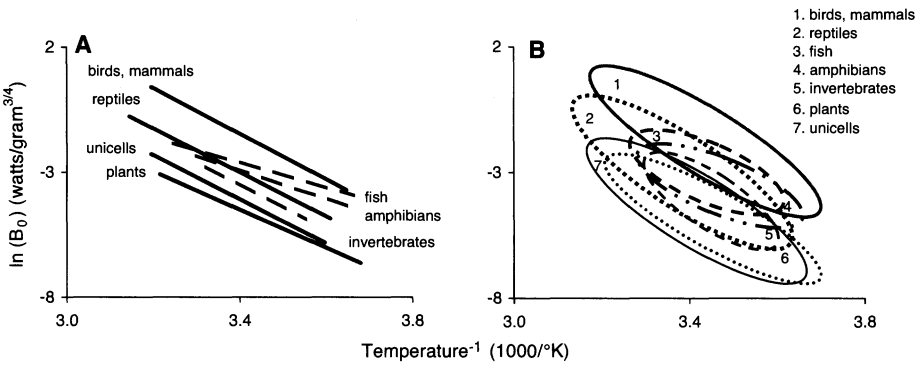

Fig. 3. A summary of the effect of temperature (1000/K) on mass-normalized resting metabolic rate (B_0, in W/g$^{3/4}$) for organisms from Fig. 1. (**A**) The regression lines are fit to the data in Fig. 1. Dashed and solid lines represent those groups listed on the right and left sides of the figure, respectively. (**B**) The envelopes are drawn around the data points for groups in Fig. 1.

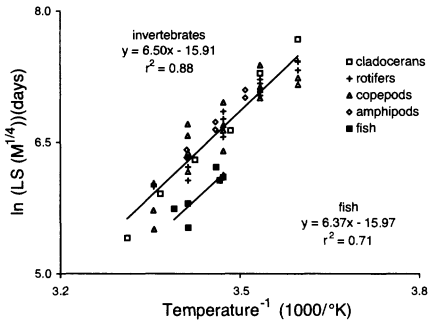

Fig. 2. Effects of body mass (M, in g) and temperature (1000/K) on life-span (LS, in days) for aquatic invertebrates and fish held at different constant temperatures in the laboratory. Data sources listed at *Science* Online (*7*).

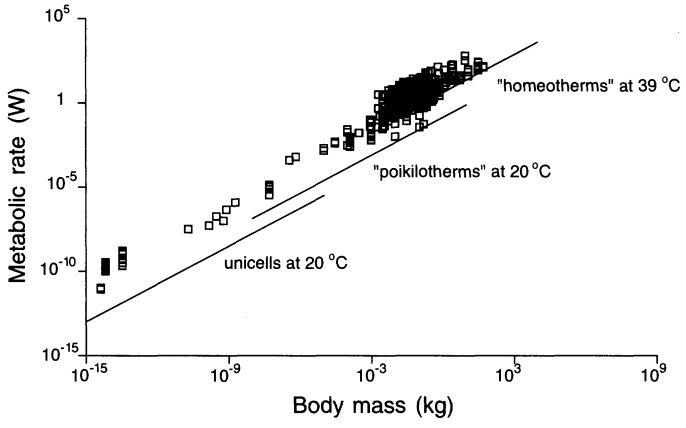

Fig. 4. A comparison of the temperature-standardized relation for whole-organism metabolic rate (W) as a function of body mass (kg) obtained in this study with the depiction of Hemmingsen (*1*). Data points represent unicells, plants, ectotherms, and endotherms from Fig. 1, all standardized to 20°C. The three lines represent the relations obtained by Hemmingsen for unicells, ectotherms ("poikilotherms"), and endotherms ("homeotherms").

This allows a comparison of temperature-standardized resting metabolic rates with Hemmingsen's classical study (*1*) (Fig. 4). Hemmingsen's work implies that ectotherms, endotherms, and unicells have distinctively different, nonoverlapping metabolic allometries. He argues that this suggests three major steps in the evolution of animal metabolism. The data in Fig. 4 show that this is an oversimplification. Temperature-standardized metabolic rates do not differ among unicells, invertebrates, and plants, but the rates for ectothermic vertebrates (fishes, amphibians, and reptiles) are slightly higher, and the rates for endothermic birds and mammals are slightly higher still. So instead of these groups having no overlap and differing by a factor of approximately 225 as suggested by Hemmingsen, there is extensive overlap with the average metabolic rates of unicells and plants separated from those of birds and mammals by about 20-fold.

Thus, metabolic rate—the rate at which organisms transform energy and materials—is governed largely by two interacting processes: the Boltzmann factor, which describes the temperature dependence of biochemical processes, and the quarter-power allometric relation, which describes how biological rate processes scale with body size. Here we show that using Q_{10} can introduce substantial error and that the temperature dependence of metabolic rate is relatively constant across a range of temperatures from 0 to 40°C. Application of the UTD to data on biological rate processes should reveal when the observed variation in response to temperature can be explained parsimoniously by Eq. 1, and when some additional biological mechanism is required. Emphasis on how metabolic rates depend primarily on body size and temperature promises to contribute to understanding how microbes, plants, and animals control the fluxes and storage of energy and materials on scales from local ecosystems to the biosphere (*13*, *14*).

References and Notes

1. A. M. Hemmingsen, *Rep. Steno Mem. Hosp. and Nordisk Insulin Laboratorium* **9**, 6 (1960).
2. M. Kleiber, *Hilgardia* **6**, 315 (1932).
3. G. B. West, B. J. Enquist, J. H. Brown, *Nature* **398**, 573 (1998).
4. G. B. West, J. H. Brown, B. J. Enquist, *Science* **276**, 122 (1997).
5. R. A. H. Vetter, *J. Comp. Physiol. B* **165**, 46 (1995).
6. J. A. Raven, R. J. Geider, *New Phytol.* **110**, 441 (1988).
7. Metabolic rates were measured as resting rates using oxygen consumption in animals and unicells, and oxygen consumption or carbon dioxide production in plants. A respiratory coefficient of 1 was used to convert CO_2 production to O_2 consumption in plants. A density of 1.43 g/l for O_2 and 1.97 g/l for CO_2 was used to convert various units to ml/hour. A factor of 0.335 W/g was used to convert ml/hour to W/$g^{3/4}$. Unicell mass was sometimes estimated from volume using a density of 1 g/ml. Metabolic rates of fish were stipulated as standard rates. Sources for all data presented in this paper, and statistics for regressions presented in Web fig. 1 and table 1 are available on *Science* Online at www.sciencemag.org/cgi/content/full/293/5538/2248/DC1.
8. K. A. Nagy, *Ecol. Monogr.* 57, 111 (1987).
9. A. J. Hulbert, P. L. Lewis, *Annu. Rev. Physiol.* **62**, 207 (2000).
10. K. J. Niklas, B. J. Enquist, *Proc. Natl. Acad. Sci. U.S.A.* **98**, 2922 (2001).
11. F. Geizer, *J. Comp. Physiol. B* **158**, 25 (1988).
12. Metabolic rates in Fig. 4 were standardized to 20°C using the equation: $B/M_{20C} = B/M_t e^{\alpha(1/20-1/t)}$ where t is body temperature and α is the slope of the line for each species group from Fig. 1.
13. R. B. Rivken, L. Legendre, *Science*, **291**, 2398 (2001).
14. R. Valentini *et al.*, *Nature*, **404**, 861 (2000).

15. J.F.G., G.B.W., and J.H.B. are grateful for the support of the Thaw Charitable Trust and a Packard Interdisciplinary Science Grant; V.M.S., for the support of the National Science Foundation; and E.L.C., for the support received as a MacArthur Fellow. All are grateful to William Woodruff for discussions. Lastly, J.F.G. acknowledges the support and encouragement received from R. J. Gillooly.

25 April 2001; accepted 1 August 2001

A Circadian Output in *Drosophila* Mediated by *Neurofibromatosis-1* and Ras/MAPK

Julie A. Williams,[1,2] Henry S. Su,[1,2] Andre Bernards,[4] Jeffrey Field,[3] Amita Sehgal[1,2]*

Output from the circadian clock controls rhythmic behavior through poorly understood mechanisms. In *Drosophila*, null mutations of the *neurofibromatosis-1* (*Nf1*) gene produce abnormalities of circadian rhythms in locomotor activity. Mutant flies show normal oscillations of the clock genes *period* (*per*) and *timeless* (*tim*) and of their corresponding proteins, but altered oscillations and levels of a clock-controlled reporter. Mitogen-activated protein kinase (MAPK) activity is increased in *Nf1* mutants, and the circadian phenotype is rescued by loss-of-function mutations in the Ras/MAPK pathway. Thus, *Nf1* signals through Ras/MAPK in *Drosophila*. Immunohistochemical staining revealed a circadian oscillation of phospho-MAPK in the vicinity of nerve terminals containing pigment-dispersing factor (PDF), a secreted output from clock cells, suggesting a coupling of PDF to Ras/MAPK signaling.

The endogenous circadian pacemaker controls the daily oscillations of both cellular and behavioral processes and can be entrained to environmental cues such as light and maintain daily cycling in the absence of such cues. The molecular components of the circadian clock form a perpetually oscillating 24-hour feedback loop (*1*). The signaling mechanism that mediates output from these clock proteins to behavior is not known, although a secreted neuropeptide, PDF, may be a crucial output element in *Drosophila* (*2*).

We sought to identify other output signaling components by testing candidate molecules. One of these, the *neurofibromatosis-1* (*Nf1*) gene product neurofibromin, is highly conserved between humans and flies, with sequence similarity throughout the length of the protein (*3*). In humans, *Nf1* is a tumor suppressor. Neurofibromin inactivates the Ras oncogene through hydrolysis of guanosine triphosphate (GTP) (*4*) and lack of neurofibromin expression in humans causes neurofibromatosis type 1 (NF-1). *Nf1*-deficient flies share some phenotypes with the human counterpart: Mutant flies are small (*3*), and short stature is a feature of some NF-1 patients (*5*). *Nf1* humans, flies, and mice all show learning deficits (*5–7*). The *Drosophila* neurofibromin can act as a Ras-GTPase activating protein in vitro (*3*), but no links to Ras have been demonstrated in vivo. Instead, all defects associated with mutations of the *Nf1* gene in flies are rescued by up-regulation of cyclic adenosine 3′,5′-monophosphate (cAMP)–dependent signaling. Because other defects in cAMP signaling have resulted in circadian phenotypes (*8–10*), we hypothesized that *Nf1* mutants would also exhibit abnormal circadian behavior.

To determine the effect of *Nf1* on circadian rhythms, locomotor activity in constant darkness (DD) was monitored in adult flies carrying a null mutation in the *Nf1* gene either by deletion ($Nf1^{P1}$) or by P-element insertion ($Nf1^{P2}$) (*3*). None of the $Nf1^{P1}$ flies were rhythmic [see (*11*)], and only 10% of $Nf1^{P2}$ flies displayed weak rhythms (Table 1). The parental strain, *K33*, which contains a

[1]Howard Hughes Medical Institute, [2]Center for Sleep and Respiratory Neurobiology, [3]Department of Pharmacology, University of Pennsylvania School of Medicine, Philadelphia, PA 19104, USA. [4]Massachusetts General Hospital Cancer Center, Charlestown, MA 02129, USA.

*To whom correspondence should be addressed. E-mail: amita@mail.med.upenn.edu